JACS
JOURNAL OF THE AMERICAN CHEMICAL SOCIETY
Communication
pubs.acs.org/JACS

Photostable p-Type Dye-Sensitized Photoelectrochemical Cells for Water Reduction

Zhiqiang Ji,[†] Mingfu He,[†] Zhongjie Huang,[†] Umit Ozkan,[‡] and Yiying Wu*[,†]

[†]Department of Chemistry and Biochemistry, The Ohio State University, 100 West 18th Avenue, Columbus, Ohio, 43210, United States

[‡]Department of Chemical and Biomolecular Engineering, The Ohio State University, 140 W 19th Avenue, Columbus, Ohio, 43210, United States

Supporting Information

ABSTRACT: A photostable p-type NiO photocathode based on a bifunctional cyclometalated ruthenium sensitizer and a cobaloxime catalyst has been created for visible-light-driven water reduction to produce H_2. The sensitizer is anchored firmly on the surface of NiO, and the binding is resistant to the hydrolytic cleavage. The bifunctional sensitizer can also immobilize the water reduction catalyst. The resultant photoelectrode exhibits superior stability in aqueous solutions. Stable photocurrents have been observed over a period of hours. This finding is useful for addressing the degradation issue in dye-sensitized photoelectrochemical cells caused by desorption of dyes and catalysts. The high stability of our photocathodes should be important for the practical application of these devices for solar fuel production.

Dye-sensitized photoelectrochemical cells[1] (DSPEC) represent an attractive approach for solar fuel production. In a DSPEC electrode, the light absorber is the key component that needs to sensitize a wide band gap semiconductor and is also coupled with a redox catalyst to drive the production of chemicals at the electrode. Prior DSPEC research has been predominantly focusing on photoanodes comprising chromophore-catalyst assembly for water oxidation.[2−5] By comparison, the study of dye-sensitized photocathodes for water or CO_2 reduction is rare.[6,7] Moreover, degradation of these dye-sensitized photoelectrodes due to the desorption of dye molecules[8] or the leaching of catalysts[7] has been a major issue. In order to increase their durability and efficiency, it is desirable to design dye sensitizers that bind strongly with both the oxide surface and the catalyst.

Herein we report a stable NiO photocathode based on a bifunctional cyclometalated Ru(II) sensitizer, labeled as O22 (Figure 1). On one side of the molecule, the sensitizer contains a phenylpyridyl ligand with a carboxylic acid anchoring group attached at the anionic phenyl ring. Such a design has been demonstrated to facilitate the hole injection to NiO and slow down the undesired charge recombination in our recent study of p-type dye-sensitized solar cells (p-DSSCs).[9] On the other side, the sensitizer is functionalized with a vinylpyridyl substituent at the 4,4′-bipyridine ligand allowing the axial coordination to the cobalt metal center in $CodmgBF_2$, a well-known water reduction catalyst (WRC).[10]

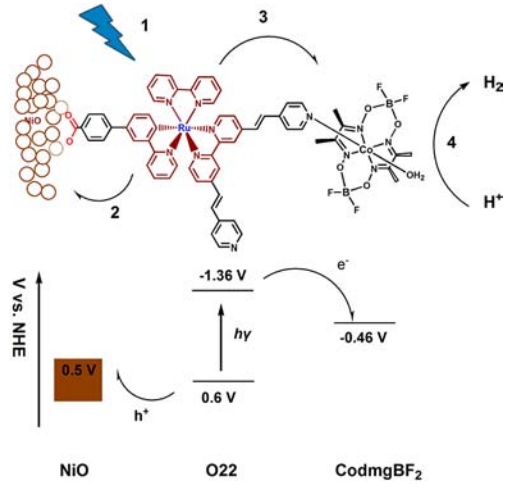

Figure 1. Schematic and energy diagram of our NiO DSPEC electrode.

Figure 1 shows the operation principle of our p-type DSPEC. A cyclometalated Ru(II) complex absorbs light (step 1) and injects holes into a p-type wide band gap semiconductor (step 2), which is opposite to the traditional n-type Gratzel cell[11] in which the sensitizers inject electrons into a n-type semiconductor. After hole injection, the reduced sensitizer will transfer electrons into the catalyst (step 3), $CodmgBF_2$, which facilitates a two-electron reduction of water to form a hydrogen molecule (step 4). The sequence of these steps is based on our prior study on the hole injection rate from a similar cyclometalated ruthenium sensitizer to NiO[9] and a recent study by Tiede et al.[12] on the axially coordinated assembly of ruthenium polypyridyl complexes and cobaloxime.

The redox potentials of our sensitizer and $CodmgBF_2$ were determined by cyclic voltammetry, and the results are shown in Table S1 and Figure S1. The oxidation potential of O22 is 0.60 V, which is more positive than VB of NiO (0.5 V).[13] Therefore the hole injection from the O22 sensitizer to NiO is thermodynamically favorable, and the first reduction potential of O22 and the redox potential of Co(II)/Co(I) in $CodmgBF_2$ are −1.36 and −0.46 V, respectively. The results indicate there

Received: May 6, 2013
Published: July 29, 2013

   dx.doi.org/10.1021/ja404525e | J. Am. Chem. Soc. 2013, 135, 11696−11699

is a large driving force for electron transfer from reduced O22 to $CodmgBF_2$.

A stable supramolecule can be formed by the axial coordination of the pyridyl group of O22 to the cobalt metal center of $CodmgBF_2$.[12,14] To confirm this, we have performed a UV−vis titration experiment to determine the binding constant by using a model compound $Ru(bpy)(ppy)(pybpy)PF_6$ (without the benzoic acid group, see SI for the structure). A distinct red shift from 571 to 593 nm and an increased absorption were observed upon the addition of $CodmgBF_2$ (Figure S2). The association constant of 2.6×10^3 M^{-1} was calculated from the Job plot of the absorption change versus the concentration of $CodmgBF_2$ (Figure S2). The results support the formation of a stable suppramolecular complex between $Ru(bpy)(ppy)(pybpy)PF_6$ and $CodmgBF_2$.

The detailed preparation of the sensitized electrodes is in the SI. UV−vis absorption spectra of the films (Figure S3) show clear evidence of adsorption of O22 on the NiO films. The XPS analysis (Figure S4) was performed on the assembled nanoparticulate film. The peak centered at 280.7 eV is consistent with Ru3d of the Ru(II) complex,[15] and the peak at 781.3 eV is consistent with Co2p of the Co(II) complex.[16] The molar ratio of Co/Ru is ∼0.1 as determined by the ICP analysis by dissolving the film using dilute HNO_3.

Stability has been a major limitation of the prior n-type DSPEC devices. A major reason is that the sensitizers anchored at TiO_2 through the carboxylic acid group quickly desorb when exposed to water.[2] The stability of our O22/NiO film in the presence of neutral water and a pH 7 phosphate buffer solution (the same electrolyte we used in our photoelectrochemical (PEC) measurements) was studied. Figure S5 shows the absorption spectra of the O22/NiO film soaked in neutral DI water. The absorption spectra show negligible changes after 140 min. The absorption spectrum of the soaked water also shows no presence of any sensitizer O22. We also tested the stability of O22/NiO in a pH 7 buffer solution. No desorption of O22 from the film was observed within 6 h (Figure S5).

We have also compared the adsorption of O22 and $Ru(bpy)_2(dcb)Cl_2$, a benchmark sensitizer in prior DSPEC studies of oxygen evolution on TiO_2 films. No desorption of O22 from the TiO_2 film was observed by soaking in neutral DI water (Figure S6), whereas $Ru(bpy)_2(dcb)Cl_2$ desorbed quickly from TiO_2 film (Figure S7) with a desorption rate constant of 6.9×10^{-4} s^{-1}, consistent with the previous observations.[17] We also found that $Ru(bpy)_2(dcb)Cl_2$ desorbs very quickly from the NiO film (figure S8). Since the following photoelectrochemical measurements were performed on the alumina coated NiO films, the stability of O22 was also studied. The results reveal the similar stability as the uncoated NiO films (Figure S9).

It has been proposed that desorption of Ru(II) sensitizers with the carboxylic acid anchoring group from TiO_2 is due to the nucleophilic attack of the surface covalently bonded carboxylic acid group by water molecules.[2] A possible explanation for the observed unusual high stability is the enhanced electron density as the carboxylic acid group in our new sensitizer is attached at the more electron-rich moiety than at bipyridine ligand in $Ru(bpy)_2(dcb)Cl_2$, which may decrease the possibility of nucleophilic attack by water. In addition, the O22/NiO electrode exhibits excellent photo stability under intense illumination in our 2.5 h chronoamperometry experiment (see Figure 4 and the related content). The superior stability of metal oxide bound chromophores is very important for the practical application of DSSCs and dye-sensitized photosynthetic cells.

The performance of our photocathodes was studied by PEC measurements. It is known that the back electron transfer between photogenerated holes in NiO and the reduced sensitizer is ultrafast,[9] which is deteriorative to the performance of p-DSSC devices. However improvement can be achieved by coating of a monolayer of alumina by the atomic layer deposition (ALD) method on the surface of the NiO film[18] due to suppressed hole−electron recombination across the NiO surface.

In this study, we first examined the influence of alumina coating on our device performance. One layer of alumina was coated on NiO film by ALD, and the films with and without alumina coating were assembled with O22 and $CodmgBF_2$ in the same manner as described. Figure 2 shows the linear sweep

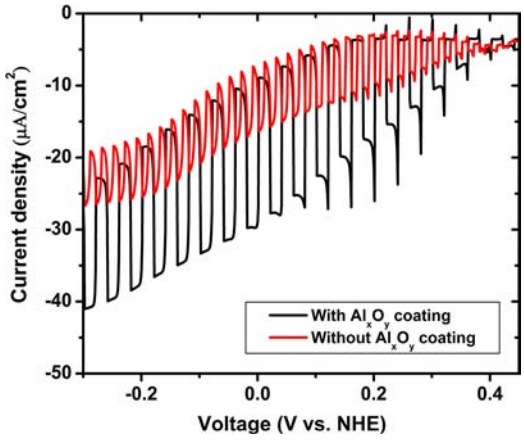

Figure 2. LSV of NiO electrode with and without alumina coating. The scan direction is from positive potential to negative potential. The scan rate is 1 mV/s.

voltammograms (LSV) of assembled photocathode with and without alumina coating. For comparison, both electrodes show similar onset potential that is close to the valence band of NiO. The electrode with alumina coating exhibits enhanced photocurrent density. The enhanced performance should be a result of reduced germinate electron−hole recombination which increases the possibility of the forward electron transfer from the reduced O22 to the $CodmgBF_2$ catalyst. As a note, all of the following measurements were performed on NiO films with one layer of alumina coating.

Next, we examined the role of $CodmgBF_2$ on hydrogen evolution. In a DSPEC device, catalysts play a very important role, which can activate the proton reduction reaction and reduce the geminate charge recombination by shifting electrons away from the semiconductor surface. The PEC measurements were performed on the electrodes with and without $CodmgBF_2$ catalysts. Figure S10 shows the LSVs of both cells. The PEC of the electrode without the cobalt catalyst yields a smaller photocurrent in comparison to that with the catalyst. Figure 3 shows the plots of photocurrent density versus applied bias. The photocurrent density was extracted from Figure S10 by subtracting the dark current from the photocurrent. The photocurrent reaches the plateau at ∼0.1 V versus NHE for both cells. When the electrode with catalyst was used as the working electrode, the onset potential is ∼0.46 V, which is an anodic shift by ∼40 mV relative to that without catalyst (0.42

dx.doi.org/10.1021/ja404525e | J. Am. Chem. Soc. 2013, 135, 11696−11699

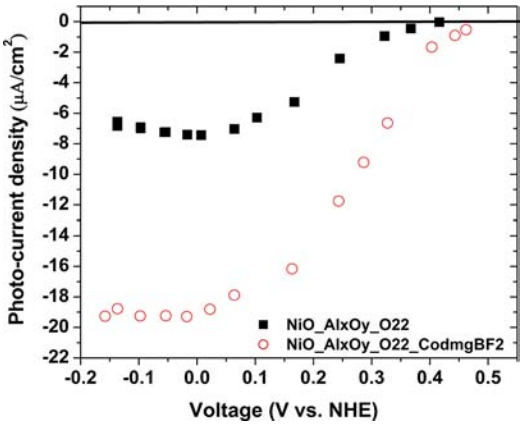

Figure 3. Plot of steady photocurrent vs applied bias for the O22-sensitized NiO with (open circles) and without (solid squares) the $CodmgBF_2$ catalyst.

V). We note that the thermodynamic potential of proton reduction at pH 7 is −0.41 V. The onset potential is very close to VB of NiO (0.5 V vs NHE), indicating $CodmgBF_2$ reduces the onset potential for proton reduction, likely due to the electron transfer from O22 sensitizer to the catalyst. We note that the NiO film loaded with only $CodmgBF_2$ gives a negligible photocurrent (Figure S11).

A noticeable feature in the LSVs (Figures 2 and S10) is that when the light illumination was turned on and off, all electrodes showed transient photocurrents at lower bias (from onset potential to ∼0.1 V). When a more negative bias is applied, the transient photocurrent gradually disappears. The transient photocurrent should be a result of accumulation of charge carriers[19] at the NiO/electrolyte interface due to either the trap of holes in the bulk of NiO or slow kinetics of proton reduction until an equilibrium is reached between proton reduction, charge recombination, and charge extraction. The sensitized NiO electrode with the $CodmgBF_2$ catalyst shows more pronounced transient photocurrent than the electrode without the catalyst (Figure S10), which suggests that the kinetics of proton reduction should not be the main factor that causes the transient photocurrent. The dependence of transient current on bias also supports that it is mainly caused by accumulation of holes in NiO, since the bias can change the local density of trap states and the transport resistance of holes in NiO. This result suggests that device performance can be improved via proper semiconductor engineering or surface treatment.

The incident-photon-to-current-conversion-efficiency spectra (IPCE) were performed on the bare NiO (a), the O22/NiO electrode (b), and the NiO electrode loaded with O22-$CodmgBF_2$ assembly (c) (Figure S12). The IPCE spectrum of the O22/NiO electrode closely matches with the absorption spectrum of O22 in the DMF solution indicating that O22 is largely responsible for photon absorption (Figure S12). It is observed that the NiO electrode loaded with O22-$CodmgBF_2$ assembly exhibits an identical spectrum shape and larger IPCE values over the whole spectrum range of 350−800 nm, confirming that the $CodmgBF_2$ catalysts can enhance the photocurrent.

One of the most intriguing features in our photocathode is that the proton reduction catalyst coordinately binds to the photosensitizer. Such a design provides the strong coupling between sensitizers and catalysts and also the high stability of the photoelectrode. To study the photo stability, a chronoamperometry of an alumina coated NiO electrode assembled with both O22 and $CodmgBF_2$ was performed under illumination at a bias of 0.1 V. The chronoamperogram is shown in Figure 4. After the initial transient spike within several

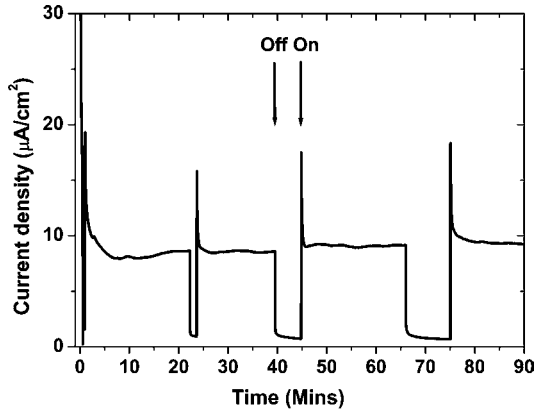

Figure 4. Chronoamperogram of the alumina coated NiO electrode loaded with O22 and $CodmgBF_2$ catalyst as a working electrode at a applied bias of 0.1 V versus NHE.

minutes, the photocurrent reaches a plateau at ∼8 $\mu A/cm^2$, and the photocurrent slightly increases to ∼9 $\mu A/cm^2$ after 1 h illumination. During the experiment, the illumination was intentionally blocked three times, indicated by the arrows in Figure 4. The dark current drops to nearly zero (∼800 nA/cm^2), confirming that the observed current under illumination is indeed photocurrent. The stable photocurrent indicates the high stability of our photocathode. Moreover, no sign of degradation of our photoelectrode is also evidenced by the negligible changes of absorption spectra before and after the photolysis experiments (Figure S13). The superior stability of our photoelectrode is a combined result of high stability of O22/NiO film toward water hydrolysis and the strong binding between O22 and the $CodmgBF_2$ catalyst.

Hydrogen generation was measured by gas chromatography (GC) with a pulsed discharge helium ionization detector. The PEC measurements were performed under a bias of −0.2 V for 2.5 h. The GC was calibrated by electrolysis with a platinum mesh electrode in our PEC electrochemical cell independently. The detail of the GC calibration curve is shown in Figure S14. After PEC, 250 ul gas at headspace was taken and measured. A calculated amount of 0.29 μmol H_2 was produced with 0.123 C of cathodic charge within the sampling time, which corresponds to 45% faraday efficiency. As shown in Figure 2, there is a significant fraction of dark current in the total current under a bias of −0.2 V, which is a major factor that contributes to the other 55% of the total current. In order to decrease the dark current, another measurement was conducted under an applied bias of 0.1 V for 2.5 h and obtained an enhanced Faraday efficiency of 68%. We note that the Faraday efficiency of 68% represents the lower limit. Under our current H_2 detection condition, the headspace gas was taken out and transported to the GC instrument. A certain amount of loss during the sample-handling process is another factor for the low Faraday efficiency.

In conclusion, we report on a photostable NiO photocathode that can be used in a PEC device for hydrogen production from water. The electrode was assembled with a cyclometalated ruthenium sensitizer and a cobaloxime catalyst. Stable photo-

dx.doi.org/10.1021/ja404525e | J. Am. Chem. Soc. 2013, 135, 11696−11699

current is produced using this photocathode, and we found that both alumina coating and cobaloxime catalyst assembled on the electrode surface can enhance the magnitude of photocurrent. Furthermore we found the cyclometalated ruthenium sensitizer O22 can bind strongly to metal oxide in the presence of neutral water and pH 7 buffer solutions. The unprecedented stability of our dye-sensitized photocathode should be important for the practical application of these devices in solar fuel production. Future effort will be focused on looking for more active WRC catalysts, assemblies, and a more efficient catalyst loading to further enhance the device performance.

■ ASSOCIATED CONTENT

Supporting Information

Detailed methods and results including synthesis, characterization of O22, PEC methods, and GC measurement of H_2, etc. This material is available free of charge via the Internet at http://pubs.acs.org.

■ AUTHOR INFORMATION

Corresponding Author

wu@chemistry.ohio-state.edu

Notes

The authors declare no competing financial interest.

■ ACKNOWLEDGMENTS

We acknowledge support from the U.S. Department of Energy, Office of Basic Energy Sciences, Division of Materials Science and Engineering under award DE-FG02-07ER46427. Y.W. thanks the research gift from Honda Research Institute, Inc.

■ REFERENCES

(1) Song, W.; Chen, Z.; Glasson, K.; Hanson, C. R. K.; Luo, H.; Norris, M. R.; Ashford, D. L.; Concepcion, J. J.; Brennaman, M. K.; Meyer, T. *ChemPhysChem* **2012**, *13*, 2882.
(2) Youngblood, W. J.; Lee, S.; Kobayashi, Y.; Hernandez-Pagan, E. A.; Hoertz, P. G.; Moore, T. A.; Moore, A. L.; Gust, D.; Mallouk, T. E. *J. Am. Chem. Soc.* **2009**, *131*, 926.
(3) Brimblecombe, R.; Koo, A.; Dismukes, G. C.; Swiegers, G. F.; Spiccia, L. *J. Am. Chem. Soc.* **2010**, *132*, 2892.
(4) Li, L.; Duan, L.; Xu, Y.; Gorlov, M.; Hagfeldt, A.; Sun, L. *Chem. Commun.* **2010**, *46*, 7307.
(5) Song, W.; Brennaman, M.; Concepcion, J.; Jurss, J.; Hoertz, P.; Luo, H.; Chen, C.; Hanson, K.; Meyer, T. *J. J. Phys. Chem. C* **2011**, *115*, 7081.
(6) Tong, L.; Iwase, A.; Nattestad, A.; Bach, U.; Weidelener, M.; Götz, G.; Mishra, A.; Bäuerle, P.; Amal, R.; Wallace, G. G.; Mozer, A. *J. Energy Environ. Sci.* **2012**, *5*, 9472.
(7) Li, L.; Duan, L.; Wen, F.; Li, C.-Y.; Wang, M.; Hagfeldt, A.; Sun, L. *Chem. Commun.* **2012**, *48*, 988.
(8) Asghar, M. I.; Miettunen, K.; Halme, J.; Vahermaa, P.; Toivola, M.; Aitola, K.; Lund, P. *Energy Environ. Sci.* **2010**, *3*, 418.
(9) Ji, Z.; Natu, G.; Huang, Z.; Kokhan, O.; Zhang, X.; Wu, Y. *J. Phys. Chem. C* **2012**, *116*, 16854.
(10) Dempsey, J. L.; Brunschwig, B. S.; Winkler, J. R.; Gray, H. B. *Acc. Chem. Soc.* **2009**, *42*, 1995.
(11) O' Regan, B.; Gratzel, M. *Nature* **1991**, *353*, 737.
(12) Mulfort, K. L.; Tiede, D. M. *J. Phys. Chem. B* **2010**, *114*, 14572.
(13) Boschloo, G.; Hagfeldt, A. *J. Phys. Chem. B* **2001**, *105*, 3039.
(14) Fihri, A.; Artero, V.; Razavet, M.; Baffert, C.; Leibl, W.; Fontecave, M. *Angew. Chem., Int. Ed.* **2008**, *47*, 564.
(15) Agnes, C.; Arnault, J.; Omnes, F.; Jousselme, B.; Billon, M.; Bidan, G.; Mailley, P. *Phys. Chem. Chem. Phys.* **2009**, *11*, 11647.
(16) Andreiadi, E. S.; Jacques, P.; Tran, P.; Leyris, A.; Chavarot-Kerlidou, M.; Jousselme, B.; Matheron, M.; Pecaut, J.; Palacin, S.; Fontecave, M.; Artero, V. *Nat. Chem.* **2013**, *5*, 48.
(17) Hanson, K.; Brennaman, M. K.; Luo, H.; Glasson, C. R. K.; Concepcion, J. J.; Song, W.; Meyer, T. *J. ACS Appl. Mater. Interfaces* **2012**, *4*, 1462.
(18) Natu, G.; Huang, Z.; Ji, Z.; Wu, Y. *Langmuir* **2012**, *28*, 950.
(19) Formal, F.; Tetreaul, N.; Cornuz, M.; Moehl, T.; Gratzel, M.; Sivula, K. *Chem. Sci.* **2011**, 737.